Momentum fluxes and energy dissipation in wind-forced breaking waves

Nicolò Scapin[1,2], Jiarong Wu[1,*], J. Thomas Farrar[3],
Bertrand Chapron[4], Stéphane Popinet[5] and Luc Deike[1,2]

International Ocean Vector Winds Science Team Meeting (IOVWST)
Darmstadt, Germany (May 5th - 8th, 2025)

1. Department of Mechanical and Aerospace Engineering (MAE), Princeton University, US
2. High Meadows Environmental Institute (HMEI), Princeton University, US
3. Woods Hole Oceanographic Institution (WHOI), US
4. IFREMER, Univ. Brest, CNRS, IRD, Laboratoire d'Océanographie Physique et Spatiale (LOPS), France
5. CNRS, Institut Jean Le Rond d'Alembert - Sorbonne Université, France

* Current affiliation: Courant Institute of Mathematical Sciences, New York University, US

Wind-forced breaking waves

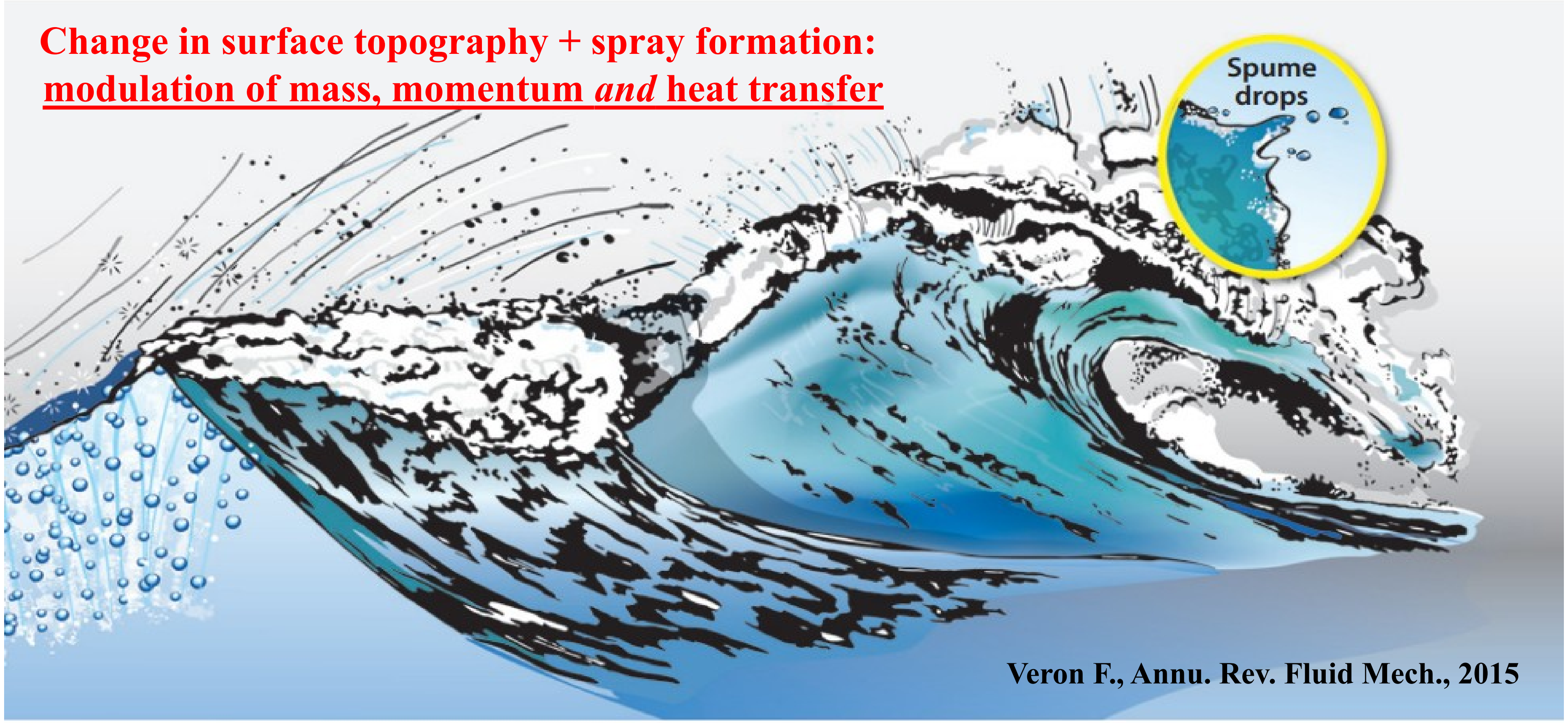

Waves and **wave breaking** modulate the exchanges
of **momentum**, **energy** and **mass** at the ocean-atmosphere interface

Using high fidelity numerical simulations to study wind-forced breaking waves

Part 1: Effect of wave breaking on momentum fluxes

→ **Scapin et al. 2025 - JFM**

Part 2: Effect of wave breaking on underwater turbulence

→ **In prep.**

Methodology:

- **Fully-resolved simulations (both in time and space) of two-phase turbulence flow**
- We solve the "native equations" (Navier-Stokes equation with surface tension) **without subgrid models or prescribed wave motion**
- **Open-source implementation** available at **http://basilisk.fr/**

Part 1: Exchanged momentum fluxes (1/2)

Dimensionless momentum flux, C_D

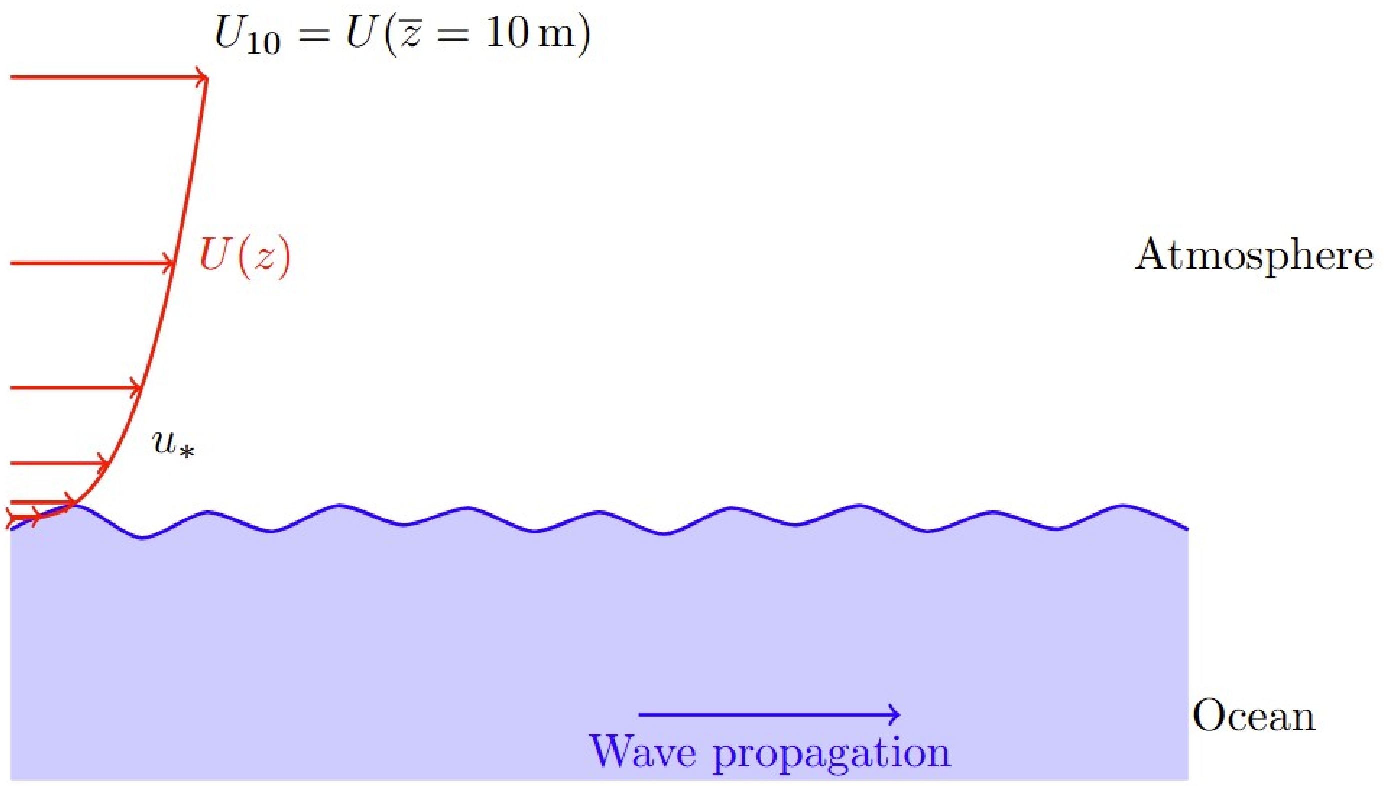

$$C_D = \frac{u_*^2}{U^2(\bar{z} = 10\ m)}$$

Drag coefficient:
the imposed stress (per unit of air density) over $\boldsymbol{U_{10}^2}$

Part 1: Exchanged momentum fluxes (2/2)

Dimensionless momentum flux, C_D

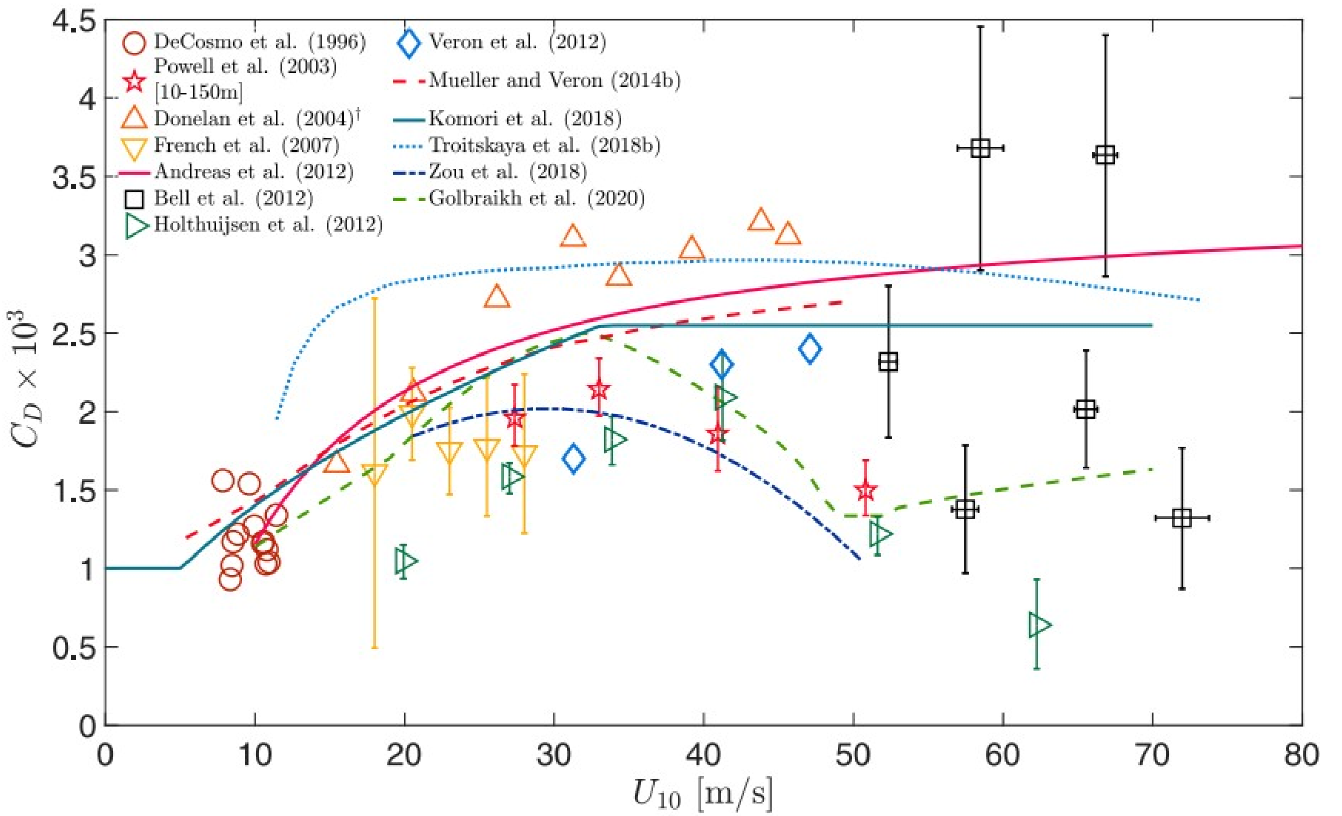

Sroka & Emmanuel (JPO, 2021)

--> $\boldsymbol{C_D}$ initially increases with $\mathbf{U_{10}}$, but at higher wind speed, it develops a saturation.

--> **Large uncertainty** and **data scattering** as U_{10} increases.

Questions:

(a) What's the **physical mechanism(s)** behind the non-linear variation of C_D with U_{10}?

(b) What's the role of **wave breaking**?

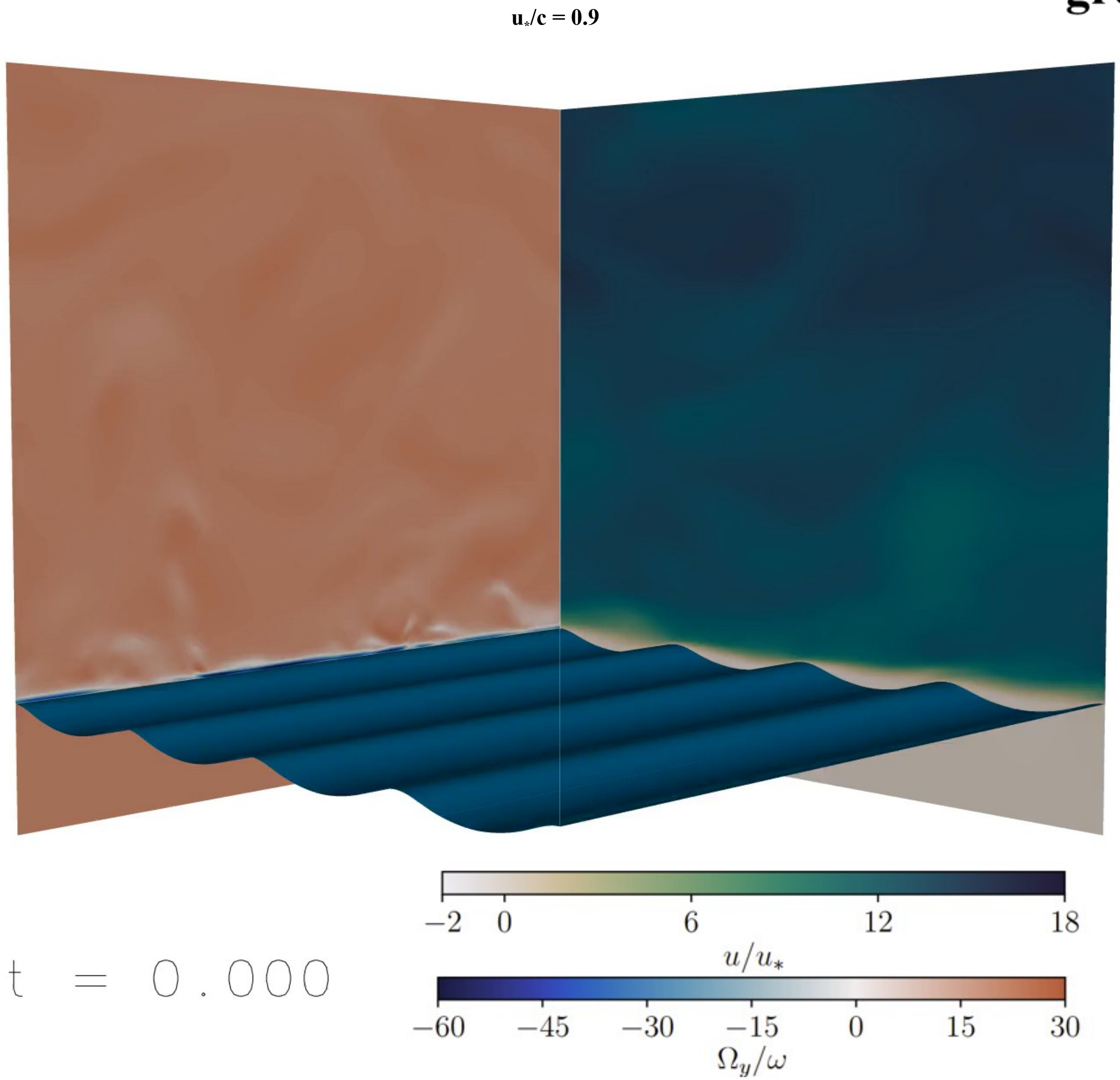

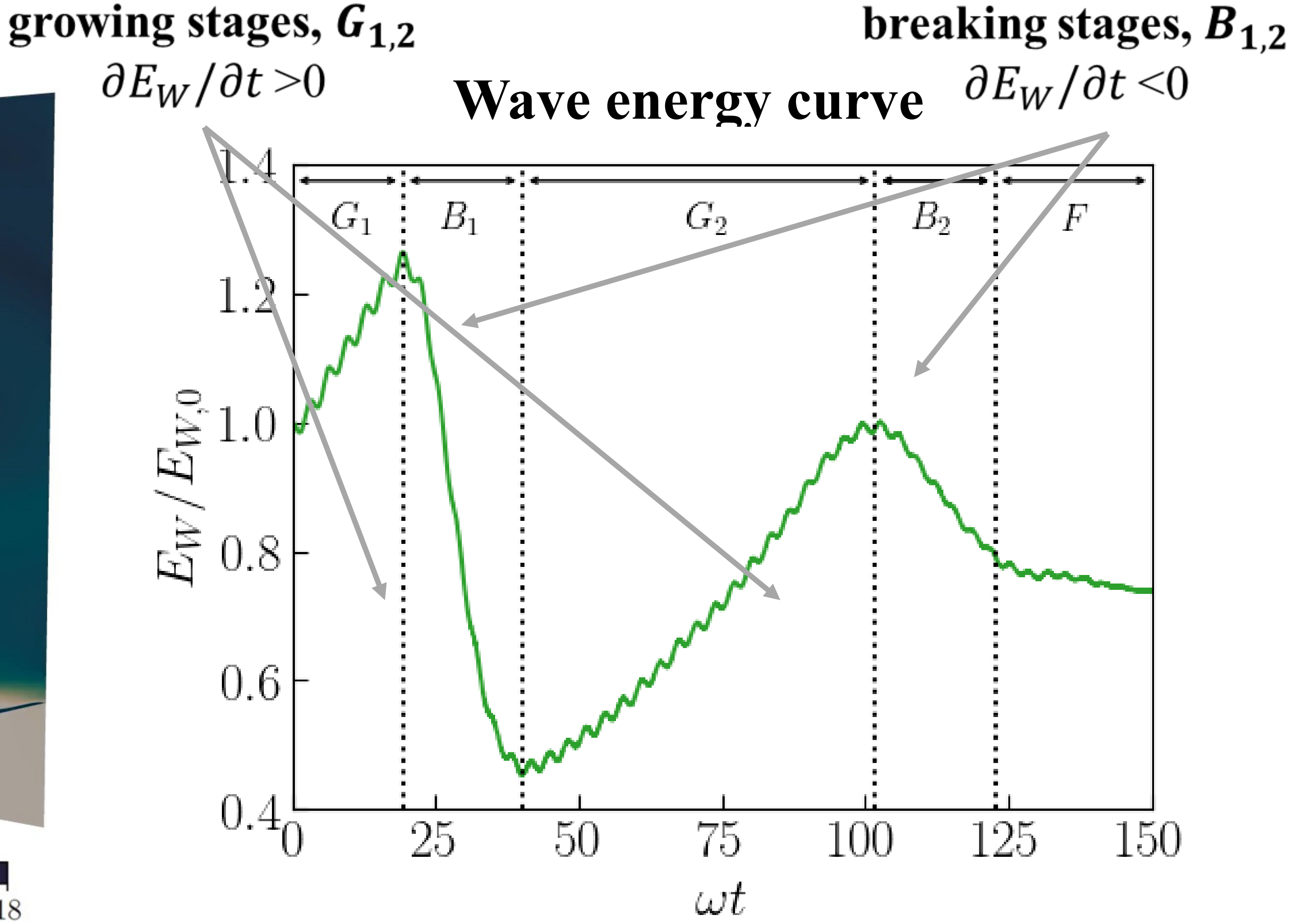

$$E_w(t) = \rho_w |\boldsymbol{g}| \int_{\Omega_w} (z - z_0) dV$$

The instantaneous change in $E_W(t)$, i.e. change in a(t)k

(1) Affects the exchanged **momentum**, i.e. ***pressure and viscous forces***, between air and water;

(2) Modulates the **airflow**;

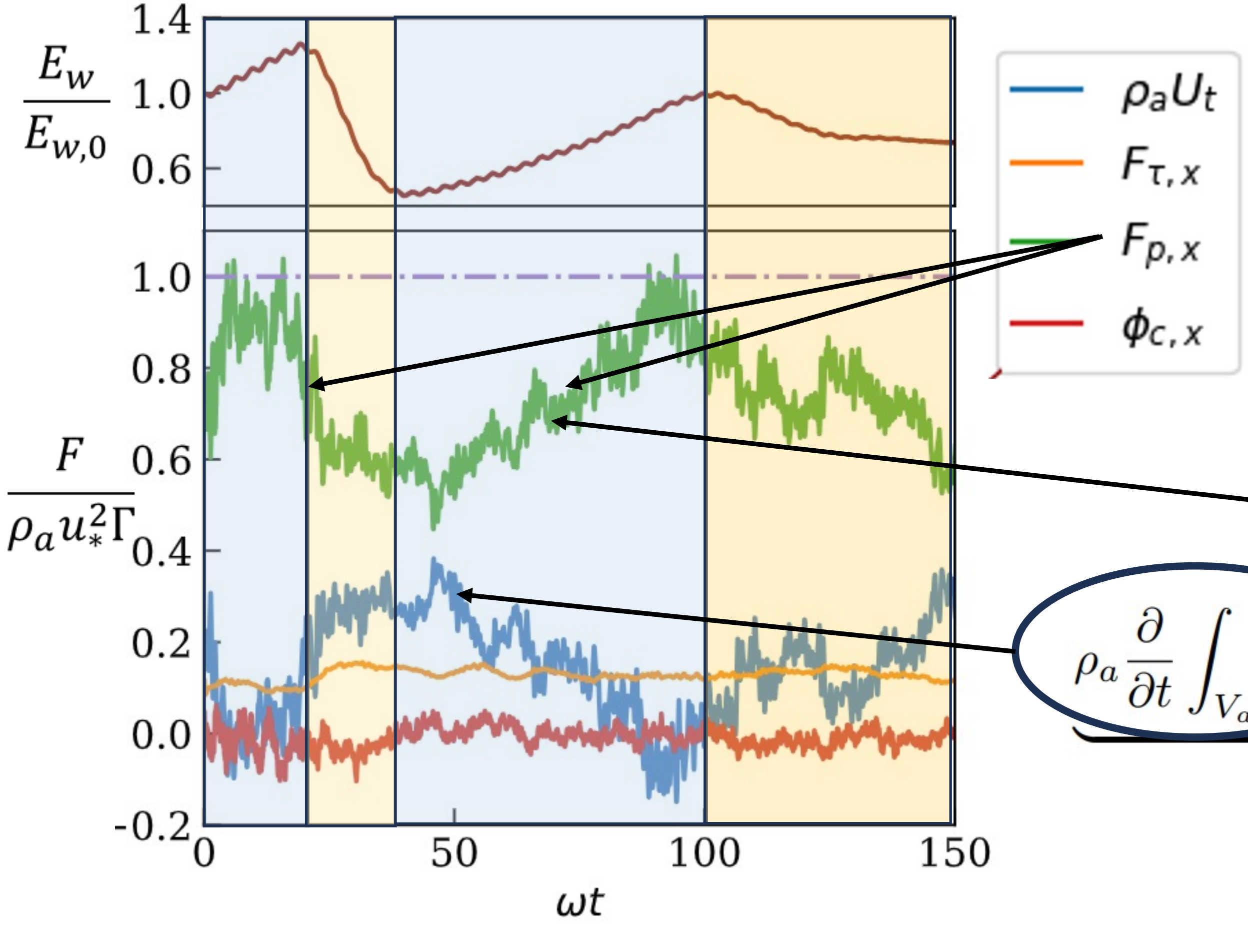

Growing stage: increase in the pressure force

Breaking stage: drop in the pressure force

Streamwise momentum budget in the air

$$\underbrace{\rho_a \frac{\partial}{\partial t}\int_{V_a} u dV - \rho_a u_*^2 \frac{V_a}{4\lambda - h_w}}_{\rho_a U_t} + \underbrace{\rho_a \int_{\Gamma} \nabla \cdot (u \mathbf{u}_{ri}) dS}_{\phi_{c,x}} = F_{p,x} + F_{\tau,x}$$

the **compensation for pressure force** comes from the change in the **mean flow** and partially from the **viscous contribution** → **Airflow modulation**

Airflow modulation

Streamwise velocity profile (in a ***wave-following coordinate***) during the **pre-breaking G_1, breaking** and **post-breaking stages $G_{2.a}$**

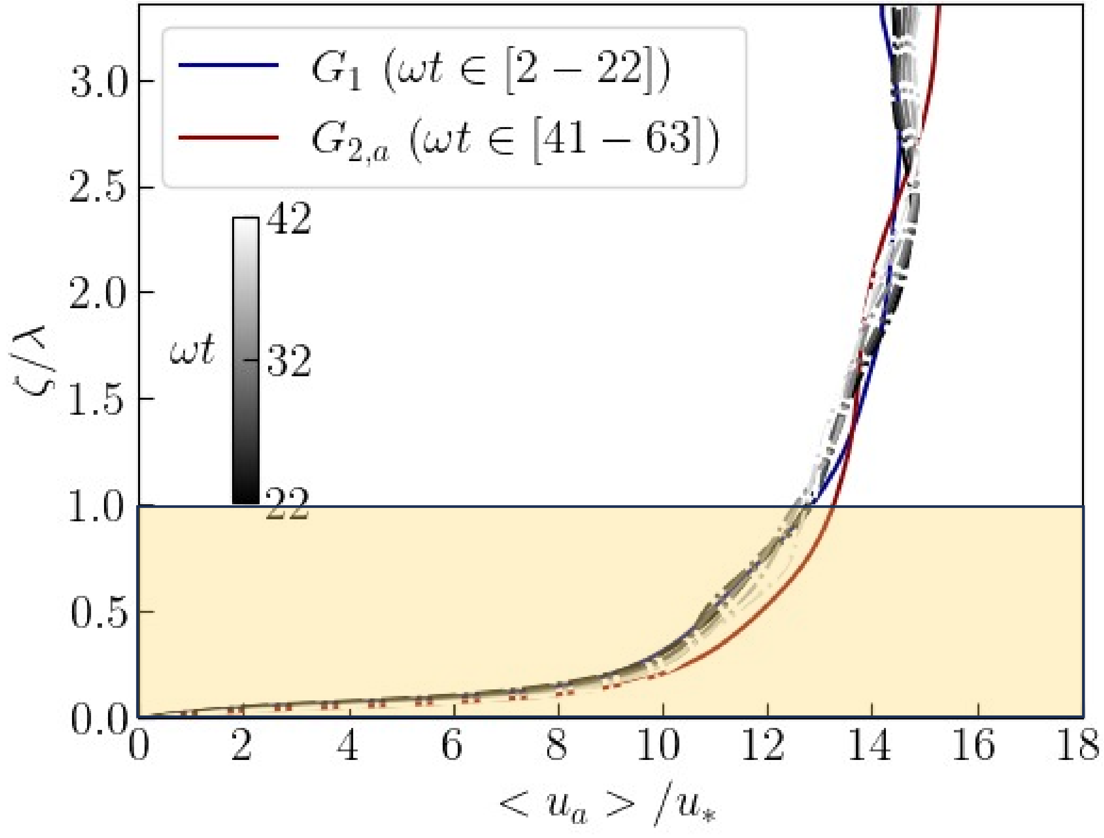

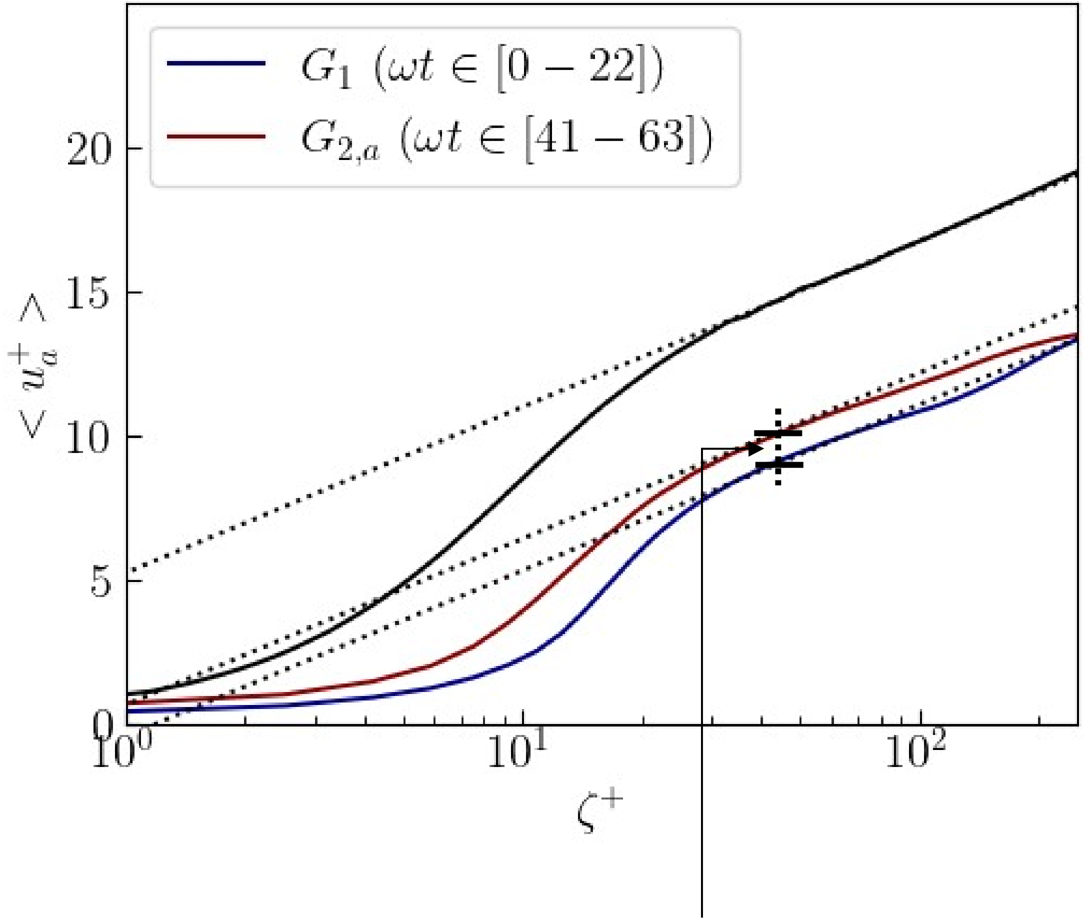

During wave-breaking the flow progressively accelerates in the region near the wave field, $\boldsymbol{\zeta < \lambda}$ → Drag reduction

During the breaking: *(1)* **reduction of the pressure force**, *(2)* **flow acceleration in the region close to the wave field**

$$C_{D,a} = \frac{2\bar{F}_p}{\rho_a \Gamma \bar{U}^2 \ (z = \frac{\lambda}{2})}$$

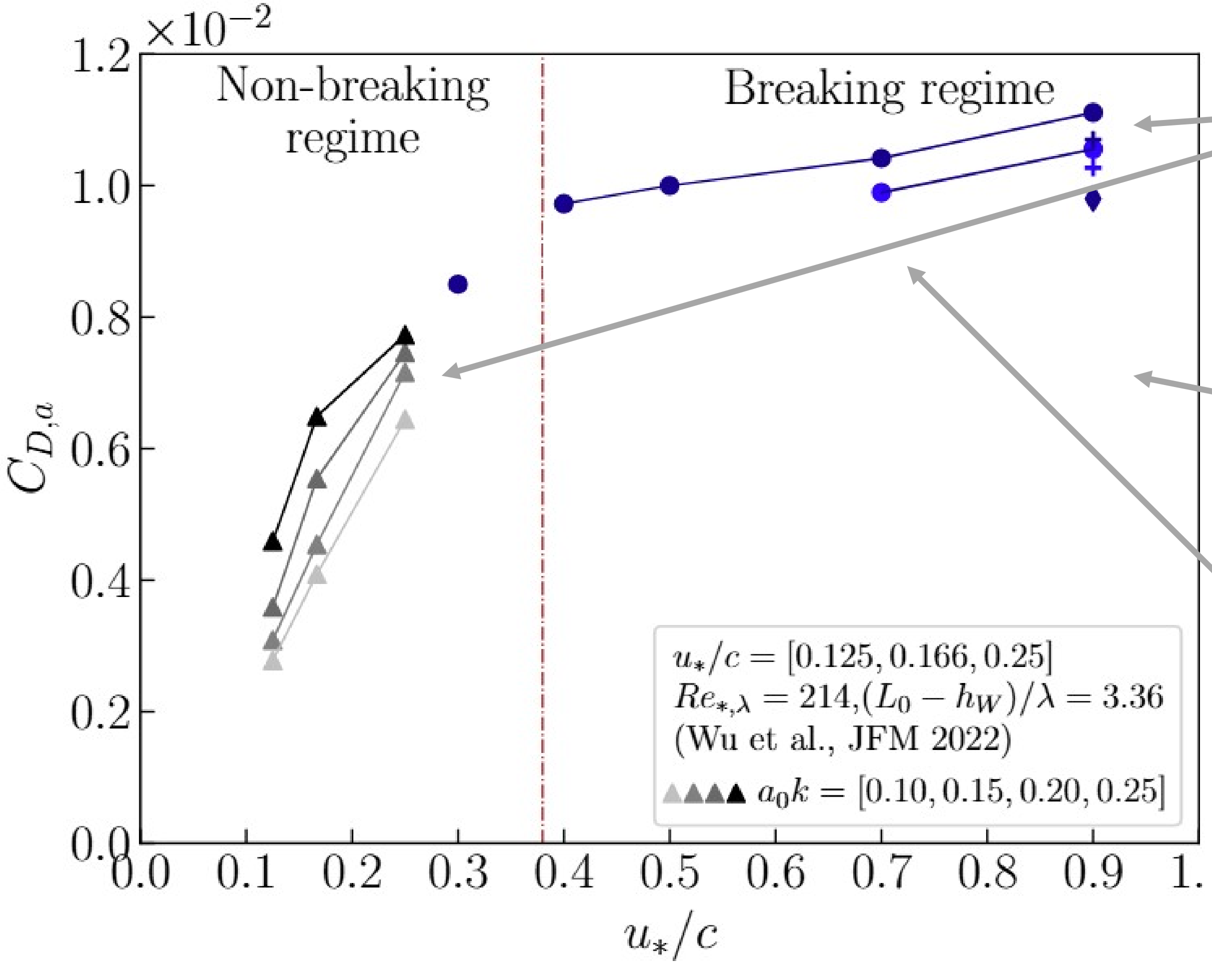

Growing stages: $C_{D,a}$ continuously increases (larger pressure force with u_*/c)

Breaking stages: during the growing stage, $C_{D,a}$ continuously increases with. During the breaking stage, $C_{D,a}$ decreases with u_*/c

Mean Saturation of $C_{D,a}$ is observed when wave breaking **is accounted for**.

Drag coefficient over breaking waves

Using the classical definition of the **drag coefficient in physical oceanography**

$$C_D = \frac{u_*^2}{U_{10}^2} \xrightarrow{U_{10}=\frac{u_*}{\kappa}\log\left(\frac{z}{z_0}\right)} C_{D,10} = \frac{\kappa^2}{\log^2\left(\frac{z=10\,m}{z_0}\right)}$$

Extracted from the velocity profile

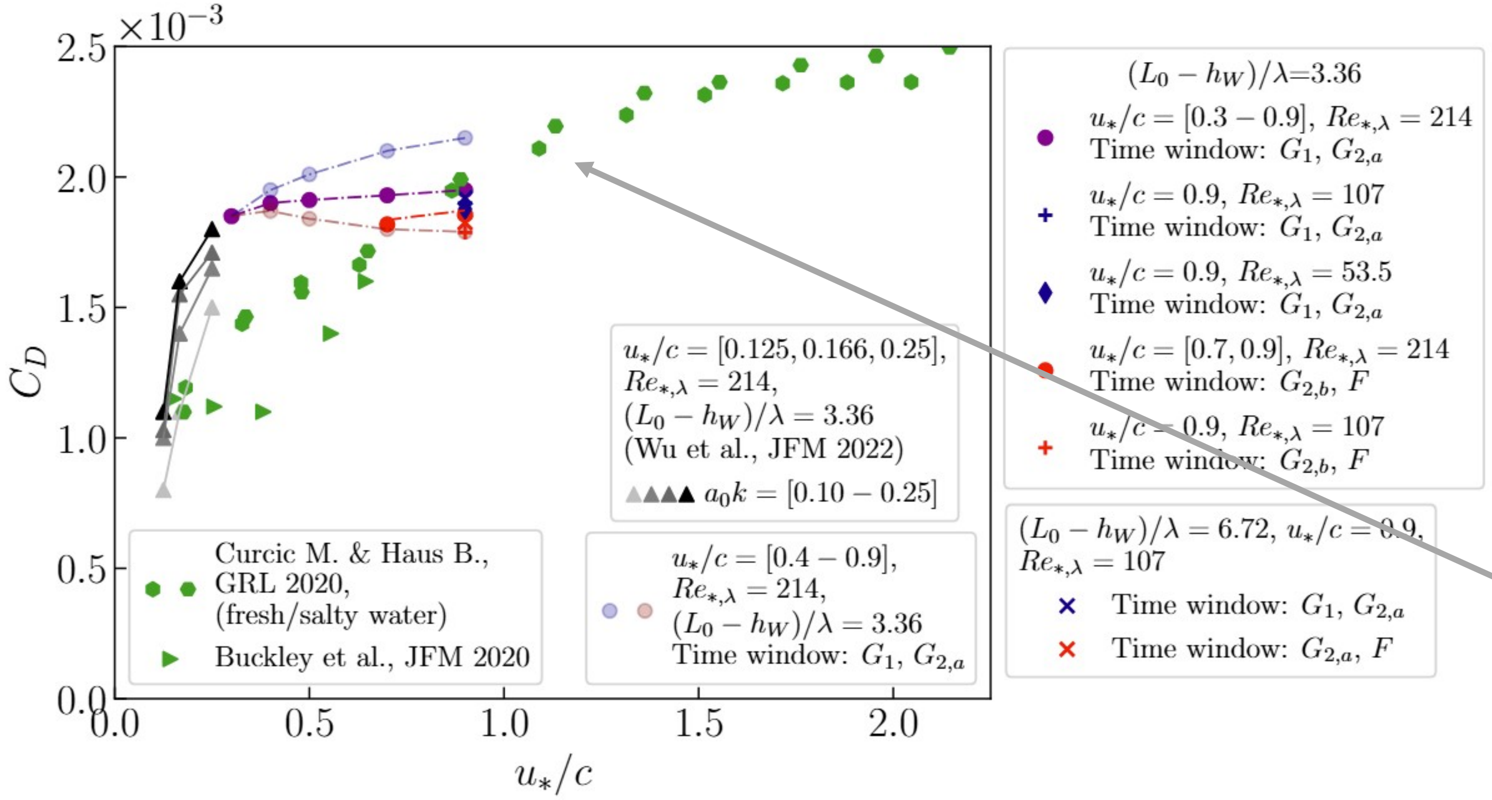

- Qualitatively similar trend to the aerodynamic drag coefficient $C_{D,A}$;
- **Drag saturation** and **reduction** occurs when the **wave breaking dynamics** is included.
- Remarkable agreement with laboratory experiments at similar u_*/c.
- **Small deviations** attributed to *(a)* multiscale nature of the wave field in the lab, *(b)* several hundreds of breaking cycles

Part 2: Wave breaking-induced dissipation

when wave break: **energy is dissipated and transfer into the water column**

Large scatter of field data for the dissipation

Enhanced turbulence dissipation

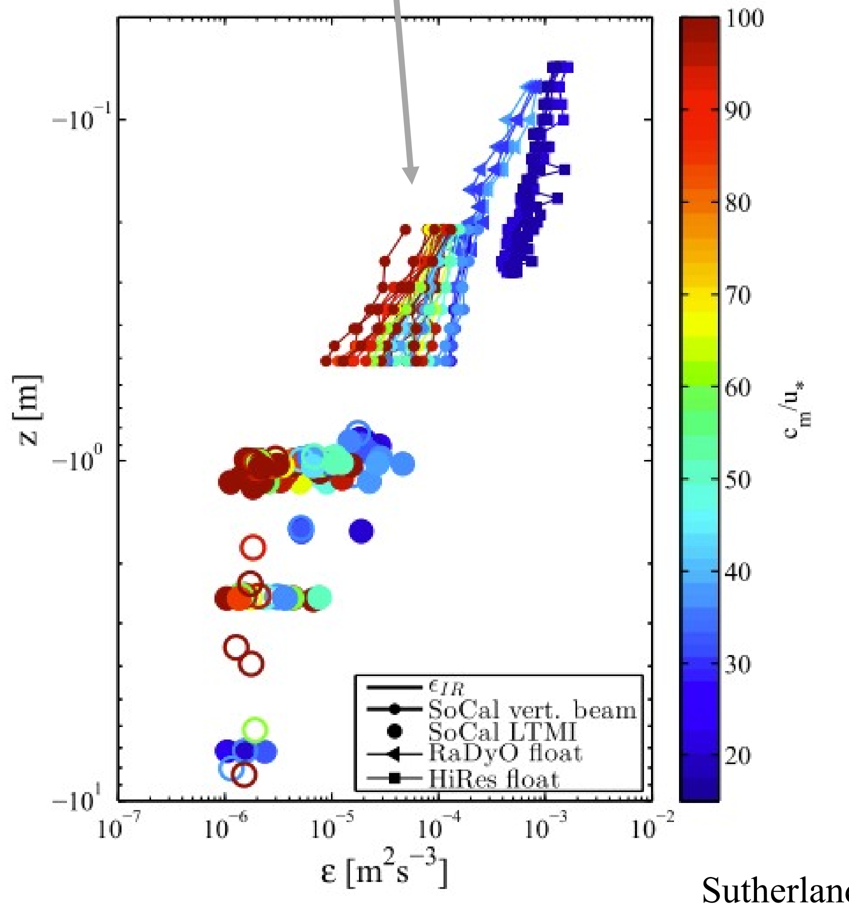

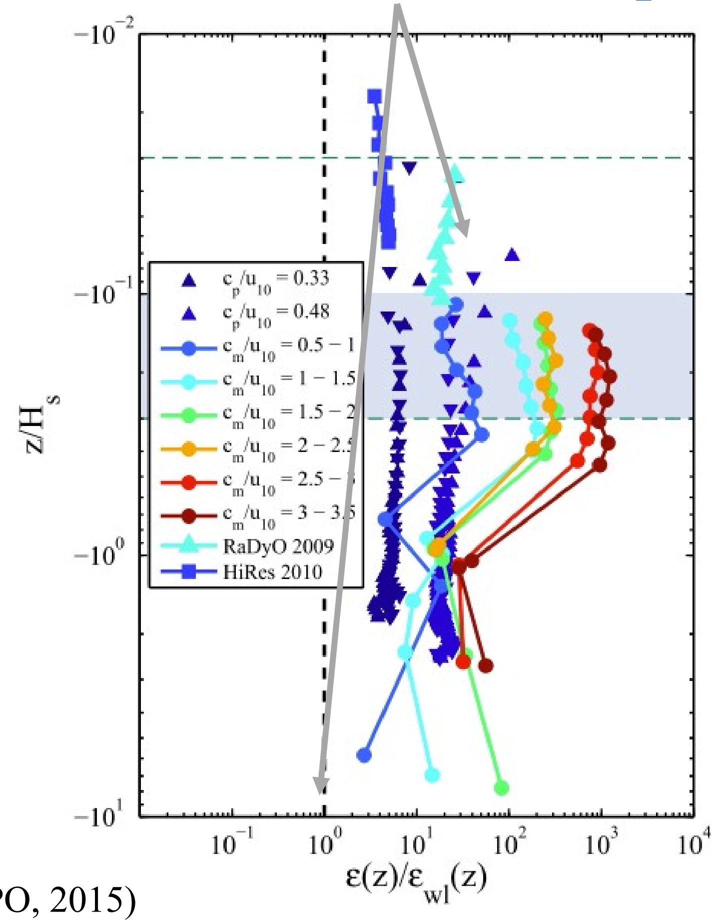

Sutherland & Melville (JPO, 2015)

How wave breaking modulate the underwater dissipation?

Wave breaking-induced dissipation (1/2)

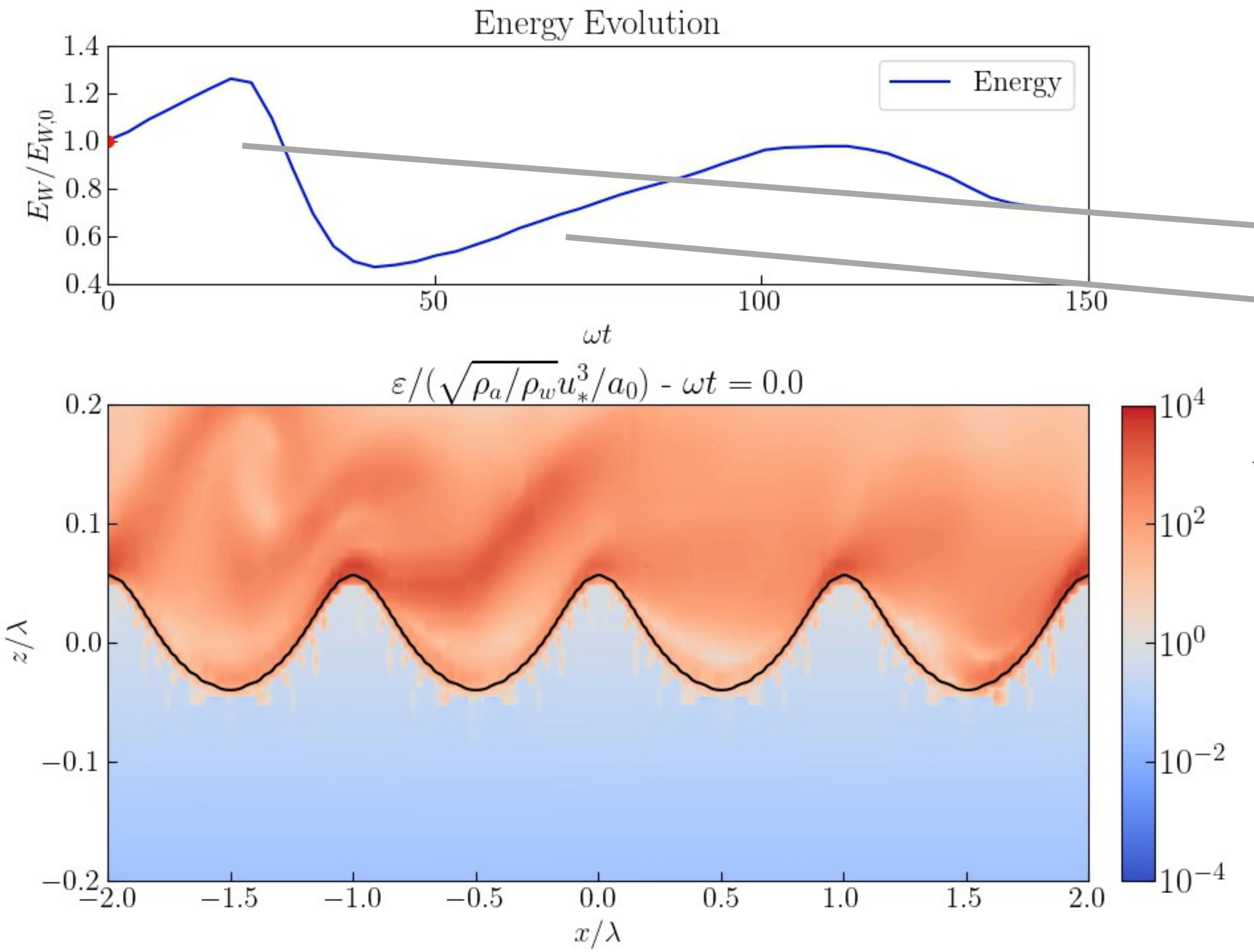

Profile during G_1, B_1 and G_2

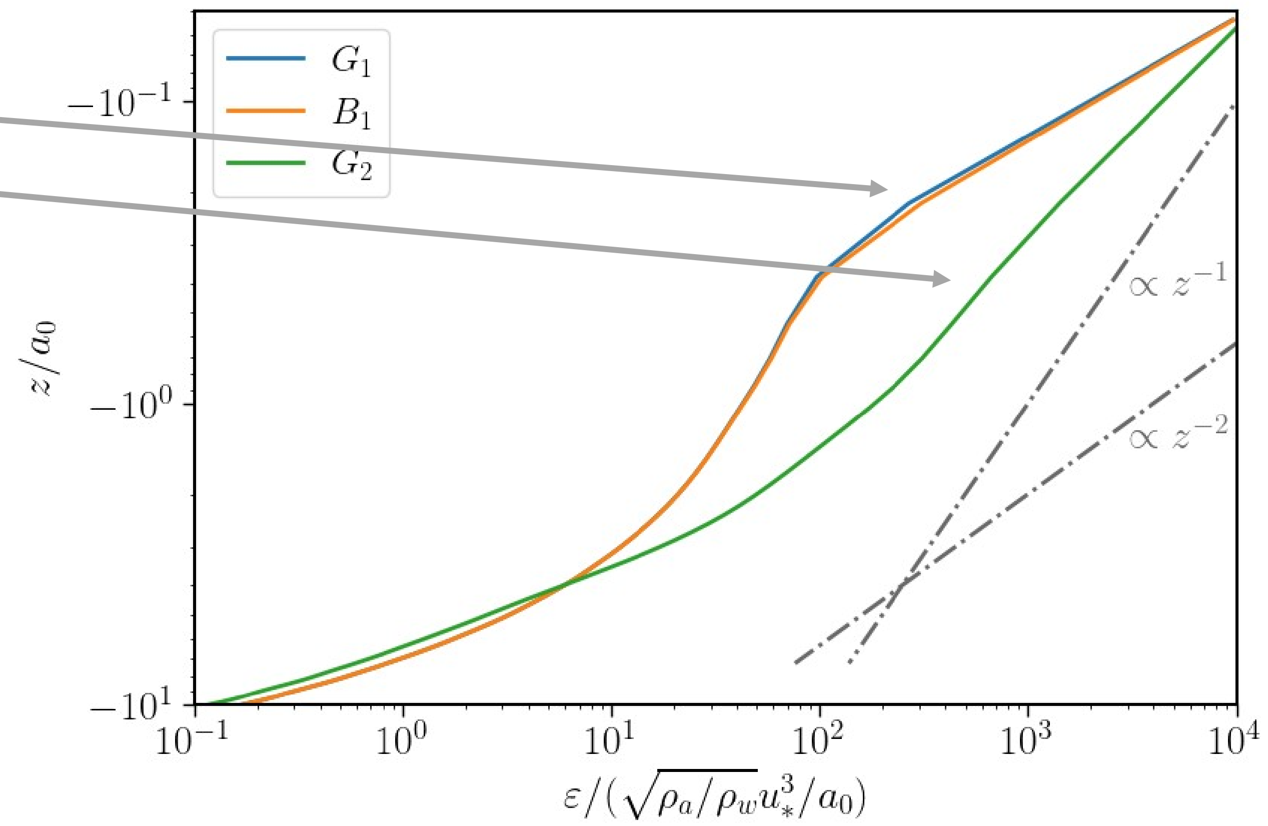

Dissipation negligible during G_1

Dissipation starts to become larger during B_1 and is transported in the water column during B_2

Wave breaking promotes the transition of the dissipation profile!

Scaling the underwater energy dissipation (1/2)

Sutherland and Melville (JPO, 2015) proposed to rescale ε as

$$\frac{\rho_w \varepsilon H_s}{S_{in}} = f\left(\frac{z}{H_s}\right)^{-1} \qquad S_{in} = F_{p,x} c \approx \rho_a u_*^2 c$$

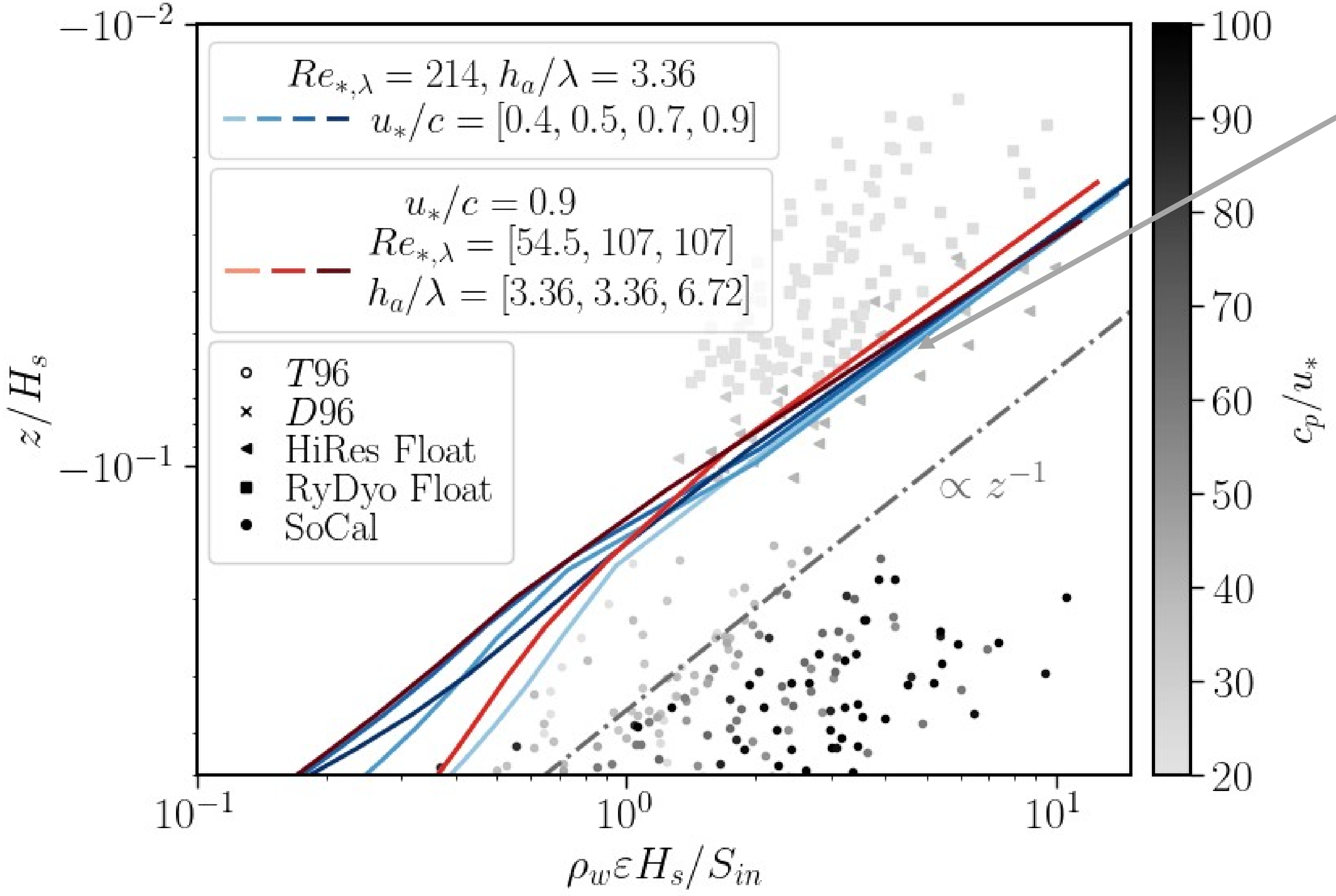

- **A good collapse** of the dissipation profiles within $0.1H_s$
- **Numerical results are compatible with the field data** at the lowest wave age near the surface
- This suggests the following scaling

$$\varepsilon_s(z) = A \frac{\rho_a}{\rho_w} \frac{u_*^2 c}{z}$$

$$A = O(1)$$

Scaling the underwater energy dissipation (2/2)

Wall-layer scaling

$$\varepsilon_{wl}(z) = u_*^3 \left(\frac{\rho_a}{\rho_w}\right)^{3/2} \frac{1}{\kappa z}$$

Proposed scaling

$$\varepsilon_s(z) = A \frac{\rho_a}{\rho_w} \frac{u_*^2 c}{z}$$

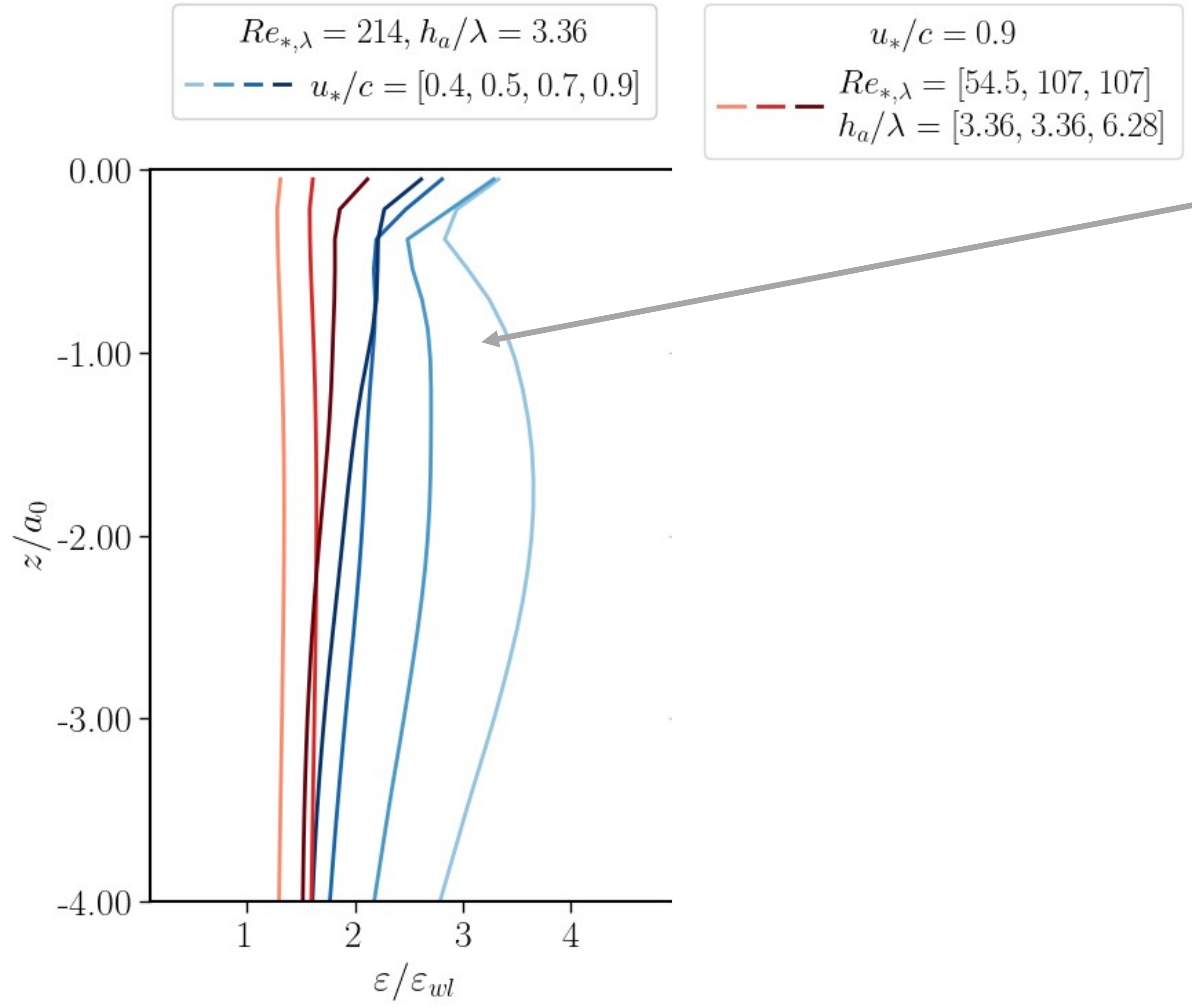

- **Wall-layer scaling:** just based on wall-layer arguments: no good collapse of the different simulation results

- **Proposed scaling** based on information from the wind, i.e. u_*, and wave field, i.e. c: good collapse across the different u_*/c

Conclusions

Momentum fluxes

- **Direct numerical simulations** of wind-forced wave breaking at high wind speed
- Analysis performed **by separating the growing** and **the breaking cycle**
- **Nonmonotonous behaviour** of the pressure force which reduces after the breaking stage (even without droplets). **Reduction is linked to the airflow modulation**
- **Saturation of $C_{D,a}$ and C_D** controlled by wave breaking dynamics

Breaking-induced dissipation

- **Wave breaking is sufficient to promote the transition of ε** to $\sim z^{-1}$
- **New scaling**, based on the **friction velocity** and **wave speed**, to unify the dissipation profile across different u_*/c

N. Scapin et al., "*Momentum fluxes in wind-forced breaking waves*", Journal of Fluid Mechanics

N. Scapin et al., "*Growth and dissipation in wind-forced breaking waves*", to be submitted in Geophysical Research Letters

High Meadows Environmental Institute
NASA
NSF
MECHANICAL & AEROSPACE ENGINEERING

Wind-wave interaction problem: physical parameters

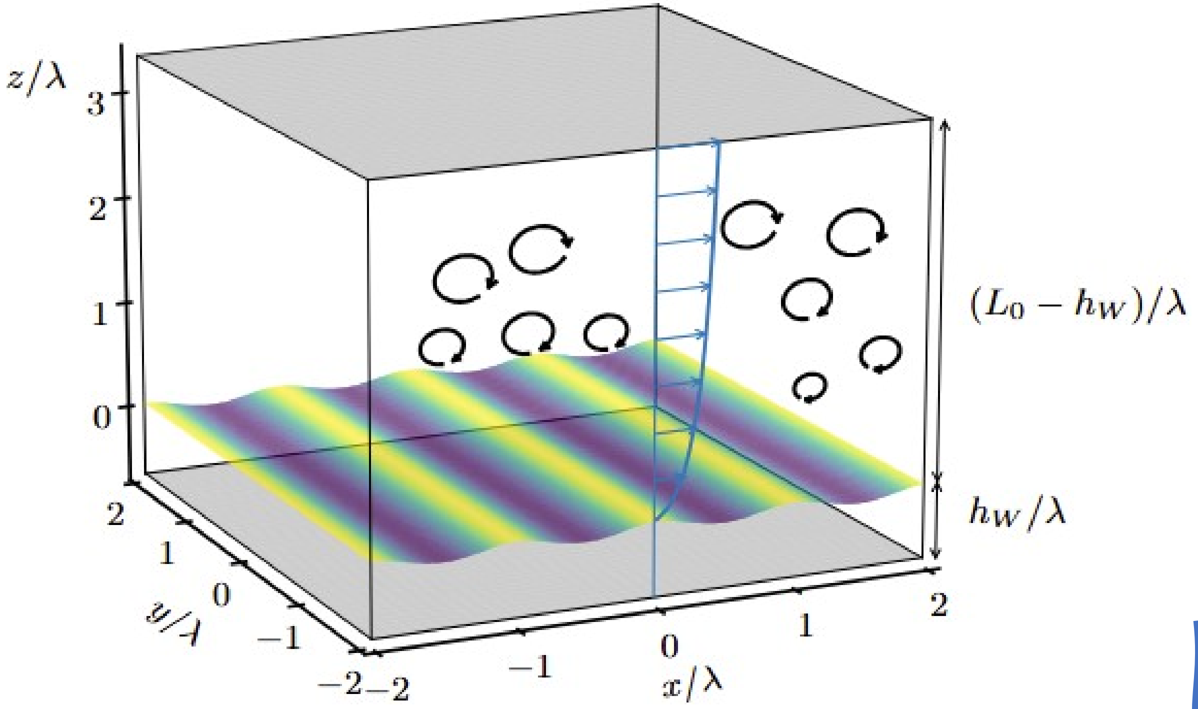

Fully-resolved direct numerical simulations using **Basilisk solver (http://basilisk.fr/)**

↓

Motion of the wave field not prescribed nor **sub-grid model for turbulence**

11 physical parameters with 3 units ([M], [L], [T])

$$\rho_a, \rho_w, \mu_a, \mu_w, (L_0 - h_W), h_W, \lambda, a_0, \sigma, |g|, u_*$$

↓ ***Π* theorem**

8 physical dimensionless parameters

- **Density ratio:** ρ_a/ρ_w
- **Ratios of length scales:** $(L_0 - h_W)/\lambda$, h_W/λ

- **Friction Reynolds number:** $Re_{*,\lambda} = \frac{\rho_a u_* \lambda}{\mu_a}$
- **Wave Reynolds number:** $Re_{wave} = \frac{\rho_w c \lambda}{\mu_w}$
- **Bond number:** $Bo = \frac{|g|(\rho_w - \rho_a)\lambda^2}{4\pi^2 \sigma}$
- **Initial wave steepness:** $a_0 k$
- **Friction velocity over wave speed:** $\frac{u_*}{c}$

Configuration set-up

- **Initial condition in Air**: fully-developed turbulence
- **Initial condition in Water**: potential flow solution of a third-order Stokes wave.

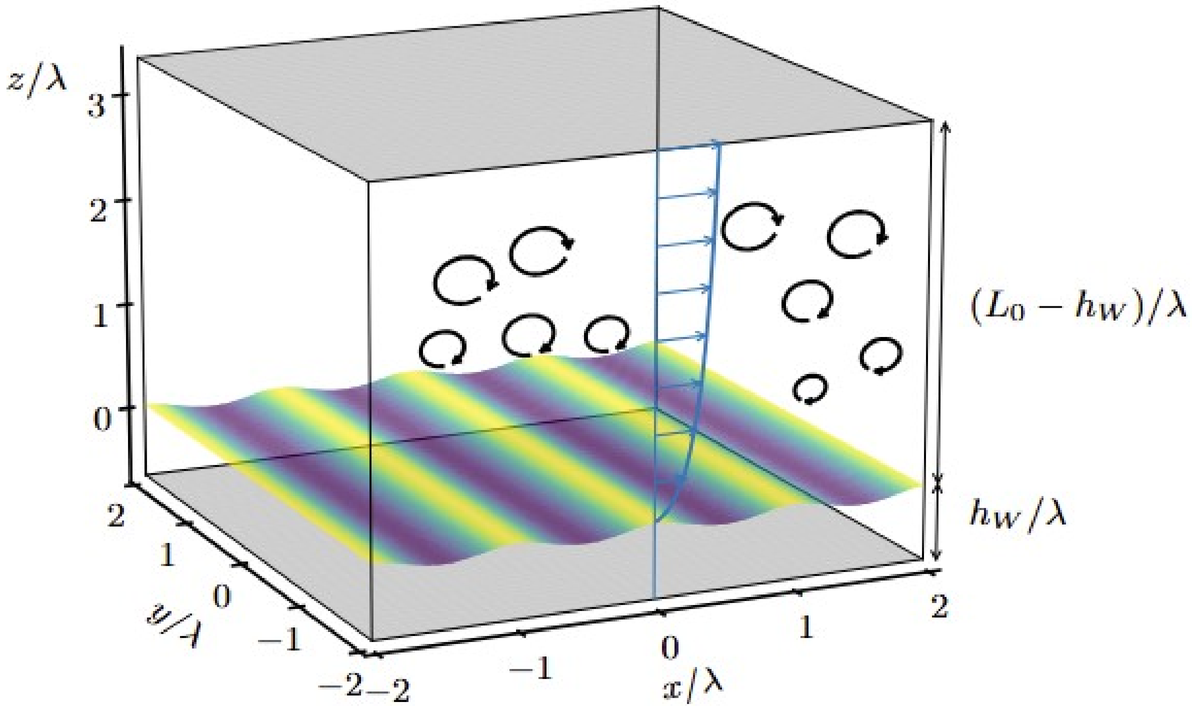

Computational domain:

- $4\lambda \times 4\lambda \times 4\lambda, h_w \approx 0.64\lambda, L_0 - h_w \approx 3.36\lambda$
- x-y: periodic directions; z: free-slip conditions;
- Grid resolution: $L^{10} - L^{11}$(i.e. $1024^3 - 2048^3$);

We fix:

$$Re_* = 720, Re_w = 2.5 \cdot 10^4, Bo = 200, a_0 k = 0.3$$

We vary (in the **high-wind speed** regime):

$$\frac{u_*}{c} = 0.3 - 0.4 - 0.5 - 0.7 - 0.9;$$

Numerical methodology

Direct solution of *(1)* continuity equation (incompressibility constraint) with *(2)* the momentum equation for a **two-phase system**

$$\nabla \cdot \boldsymbol{u} = 0$$

$$\rho\left(\partial_t \boldsymbol{u} + \nabla \cdot (\boldsymbol{u}\boldsymbol{u})\right) = -\nabla p + \nabla \cdot \left(\mu\left(\nabla \boldsymbol{u} + \nabla \boldsymbol{u}^T\right)\right) + \sigma\kappa\delta_\Gamma + \rho \boldsymbol{g}$$

Main features of the numerical algorithm:

- **Sharp-interface formulation** for the interface advection (geometric VoF)
- **Momentum consistent formulation** to ensure robustness at high density ratio
- **Well-balanced formulation** to avoid artificial parasitic currents at the interface
- **Adaptive mesh-refinement (AMR)** techniques based on wavelet transformation

Basilisk: Open-source implementation available at **http://basilisk.fr/**